Hum Genet (2007) 121:203–211
DOI 10.1007/s00439-006-0304-0

ORIGINAL INVESTIGATION

A novel gene for Usher syndrome type 2: mutations in the long isoform of whirlin are associated with retinitis pigmentosa and sensorineural hearing loss

Inga Ebermann · Hendrik P. N. Scholl · Peter Charbel Issa · Elvir Becirovic · Jürgen Lamprecht · Bernhard Jurklies · José M. Millán · Elena Aller · Diana Mitter · Hanno Bolz

Received: 2 October 2006 / Accepted: 18 November 2006 / Published online: 15 December 2006

Abstract Usher syndrome is an autosomal recessive condition characterized by sensorineural hearing loss, variable vestibular dysfunction, and visual impairment due to retinitis pigmentosa (RP). The seven proteins that have been identified for Usher syndrome type 1 (USH1) and type 2 (USH2) may interact in a large protein complex. In order to identify novel USH genes, we followed a candidate strategy, assuming that mutations in proteins interacting with this "USH network" may cause Usher syndrome as well. The *DFNB31* gene encodes whirlin, a PDZ scaffold protein with expression in both hair cell stereocilia and retinal photoreceptor cells. Whirlin represents an excellent candidate for USH2 because it binds to Usherin (USH2A) and VLGR1b (USH2C). Genotyping of microsatellite markers specific for the *DFNB31* gene locus on chromosome 9q32 was performed in a German USH2 family that had been excluded for all known USH loci. Patients showed common haplotypes. Sequence analysis of *DFNB31* revealed compound heterozygosity for a nonsense mutation, p.Q103X, in exon 1, and a mutation in the splice donor site of exon 2, c.837+1G>A. *DFNB31* mutations appear to be a rare cause of Usher syndrome, since no mutations were identified in an additional 96 USH2 patients. While mutations in the C-terminal half of whirlin have previously been reported in non-syndromic deafness (DFNB31), both alterations identified in our USH2 family affect the long protein isoform. We propose that mutations causing Usher syndrome are probably restricted to exons 1–6 that are specific for the long isoform and probably crucial for retinal function. We describe a novel genetic subtype for Usher syndrome, which we named *USH2D* and which is caused by mutations in whirlin. Moreover, this is the first case of USH2 that is allelic to non-syndromic deafness.

Electronic Supplementary Material The online version of this article (http://dx.doi.org/10.1007/s00439-006-0304-0) contains supplementary material, which is available to authorized users.

I. Ebermann · E. Becirovic · H. Bolz (✉)
Institute of Human Genetics,
University Hospital of Cologne, Kerpener Str. 34,
50931 Cologne, Germany
e-mail: hanno.bolz@uk-koeln.de

H. P. N. Scholl · P. Charbel Issa
Department of Ophthalmology,
University of Bonn, Bonn, Germany

J. Lamprecht
Department of ENT, Alfried Krupp Hospital,
Essen, Germany

B. Jurklies
Department of Ophthalmology,
University Hospital of Essen, Essen, Germany

J. M. Millán · E. Aller
Unidad de Genética, Hospital La Fe, Valencia, Spain

D. Mitter
Institute of Human Genetics,
University Hospital of Essen, Essen, Germany

Introduction

Usher syndrome, which has an estimated general prevalence of 2–6.2 in 100,000 (Ahmed et al. 2003; Keats and Corey 1999; Spandau and Rohrschneider 2002), is divided into three clinical subtypes: type 1 (USH1;

OMIM 276,900) represents the most severe subtype, with profound congenital hearing impairment, variable vestibular dysfunction, and early-onset RP. In contrast, USH2 (OMIM 276,901, 276,905, and 605,472) is characterized by moderate-to-severe stable hearing loss, normal vestibular reflexes, and onset of RP in the first to second decade. In USH3 (OMIM 276,902), which is common in the Finnish founder population but rare elsewhere, hearing loss is progressive while vestibular dysfunction and RP are variable. USH2 is probably the most frequent clinical subtype, accounting for over half of all cases (Hope et al. 1997; Rosenberg et al. 1997). In Germany, 75% of cases are clinically classified as USH2 (Spandau and Rohrschneider 2002). Mutations in the *USH2A* gene account for ≥60% of USH2 (Pennings et al. 2004). Apart from *USH3A* founder alleles in the Finnish population, USH gene founder mutations have been found to segregate in the Ashkenazi Jewish population for USH3 (p.N48K) and for USH1F (p.R245X) (Ben-Yosef et al. 2003; Ness et al. 2003), and for USH1C (c.216G>A) in the Acadian population (Bitner-Glindzicz et al. 2000; Verpy et al. 2000).

To date, eight genes for different USH subtypes have been identified: USH1B (myosin-7a; *MYO7A*), USH1C (harmonin; *USH1C*), USH1D (cadherin-23; *CDH23*), USH1F (protocadherin-15; *PCDH15*), USH1G (scaffold protein containing ankyrin repeats and a SAM domain; *SANS*), USH2A (Usherin; *USH2A*), USH2C (very large G-protein coupled receptor-1; *VLGR-1*), and USH3A (clarin-1; *USH3A*) (Ahmed et al. 2003). Several studies suggest that all known USH gene products except clarin-1 may interact in a membrane-bound supramolecular complex (Kremer et al. 2006).

In our attempt to identify new genes for Usher syndrome, we followed a candidate approach, assuming that other proteins that interact with the "USH network" may well be involved in Usher syndrome. We considered the scaffold protein whirlin an excellent candidate as recent studies suggest an interaction with several USH proteins, including MYO7A, PCDH15, CDH23, as well as the long isoforms of the USH2A and USH2C (VLGR1b) proteins (Delprat et al. 2005; van Wijk et al. 2006). Moreover, whirlin colocalizes with USH2A and VLGR1b in photoreceptor cells (synaptic regions, connecting cilium and outer limiting membrane) and hair cells (synapse, stereocilia) (Mburu et al. 2003; van Wijk et al. 2006). Here, we report a German USH2 family in which genotyping of microsatellite markers was suggestive for a causative role of the *DFNB31* gene. Both patients from this family were found to be compound heterozygous for a nonsense mutation and a splice site mutation affecting the long isoform of whirlin. This is the first description of whirlin mutations in Usher syndrome.

Materials and methods

Subjects

We clinically and genetically investigated a German family with USH2 in two siblings. Written informed consent was obtained from all participants, and the study was approved by the institutional review board of the Ethics Committee of the University Hospital of Cologne. Hearing loss was quantified by pure-tone audiometry at 125, 250, 500, 1,000, 1,500, 2,000, 3,000, 4,000, 6,000, and 8,000 Hz. Hearing loss was classified as mild (20–40 dB), moderate (41–70 dB), severe (71–95 dB), or profound (>95 dB). Vestibular function was evaluated by caloric reflex testing by electronystagmography, ENG, and by medical history concerning childhood motor development. Ocular examination included best-corrected visual acuity, slit lamp examination, and detailed stereoscopic funduscopy. Goldmann kinetic fields were obtained with the targets V4e, II4e, I4e on a standard background. Electroretinograms were measured according to the standard of the International Society for Clinical Electrophysiology of Vision (Marmor et al. 2004), beginning after 30 min of dark adaptation using 10 µs xenon flashes in a Ganzfeld bowl. Pupils were fully dilated using phenylephrine HCl (10%) and tropicamide (1%), and Burian–Allan bipolar corneal electrodes were applied after proparacaine HCl (0.5%) topical anesthesia. Retinal imaging according to standard operating procedures included fundus autofluorescence imaging with a confocal scanning laser ophthalmoscope (c-SLO-FAF, HRA-2, Heidelberg engineering, Heidelberg, Germany) and digital fundus photography (Zeiss FF4, Zeiss, Oberkochen, Germany). DNA was extracted from peripheral blood lymphocytes by standard procedures. RNA from whole blood was isolated using the PAXgene system (PreAnalytiX; Germany).

Linkage analysis

We analysed microsatellite markers specific for the USH gene loci *USH2A*, *USH2C*, *USH1B*, *USH1C*, *USH1D*, *USH1F*, *USH1G*, and *USH3A*, as well as for the *DFNB31* locus (markers were selected from the UCSC Human Genome Browser). For PCR amplification, we used fluorescent dye-labeled primers following standard conditions. Products were analysed on an

ABI-377 DNA sequencer and genotypes were determined by GeneScan software (Applied Biosystems).

Mutation analysis

For mutation analysis of the genes *MYO7A* and *DFNB31* (whirlin), we amplified coding exons using primers located in flanking intron and UTR sequences (primers were designed using ExonPrimer; Table S1). PCR amplification, PCR product purification and direct sequencing were carried out by standard conditions.

RNA analyses

Reverse transcription from total RNA was carried out with RevertAid^{TM} H Minus M-MuLV Reverse Transcriptase (Fermentas). In order to characterize the consequence of the splice site mutation c.837+1G>A, we isolated RNA from blood of the index patient and an unrelated healthy control and performed the reverse transcription reaction using oligo (dT) primers. cDNA-specific PCR amplification with FastStart Taq Polymerase (Roche) was carried out using *DFNB31*-specific primers complementary to sequences in exons 1 and 3, respectively: forward primer, 5′-gcggcgtgccaaggcccacg-3′ (exon 1), and reverse primer, 5′-ctgccttctgcttcagagcc-3′ (exon 3) (Fig. 3c). After initial denaturation at 94°C for 5 min, 30 cycles were performed which consisted of 94°C for 1 min, 65°C for 1 min, and 72°C for 1 min, with a final extension step of 72°C for 10 min. PCR products were isolated from agarose gel (PCR purification kit and QG buffer, Qiagen) and sequenced using the amplification primers.

Accession numbers

DFNB31 mRNA: GenBank NM_015404.

Results

Patients and clinical evaluation

The index patient (30 years), III:5, had been diagnosed with congenital hearing impairment. Averaged over the frequencies of 0.5, 1, 2 and 4 kHz, hearing loss is mild (Fig. 1, left). Hearing aids became necessary at the age of 13 years and sufficiently compensate for the deficit (the patient has no problems in communicating over the phone, plays guitar). Language and motor development was normal and there was no vestibular dysfunction. The index patient's eldest sister (41 years), III:1, has congenital hearing loss and was supplied with hearing aids at the age of 13 years. Hearing impairment is moderate (averaged over 0.5, 1, 2 and 4 kHz; Fig. 1, right). There is no history of noise exposure in III:5 and III:1. Non-syndromic late-onset hearing loss was reported to segregate in an autosomal dominant pattern in the family of the patients' mother, II:2. She was diagnosed with hearing loss at the age of 57 years and needed hearing aids by the age of 67 years. Hearing impairment starting at 50 years was also reported in her brother, II:3, who was supplied with hearing aids at the age of 60 years (his son, 41 years, has normal hearing). I:1 already had hearing loss at 30 years of age.

The index patient (III:5) noticed progressively impaired night vision at the age of 20 years. Best-

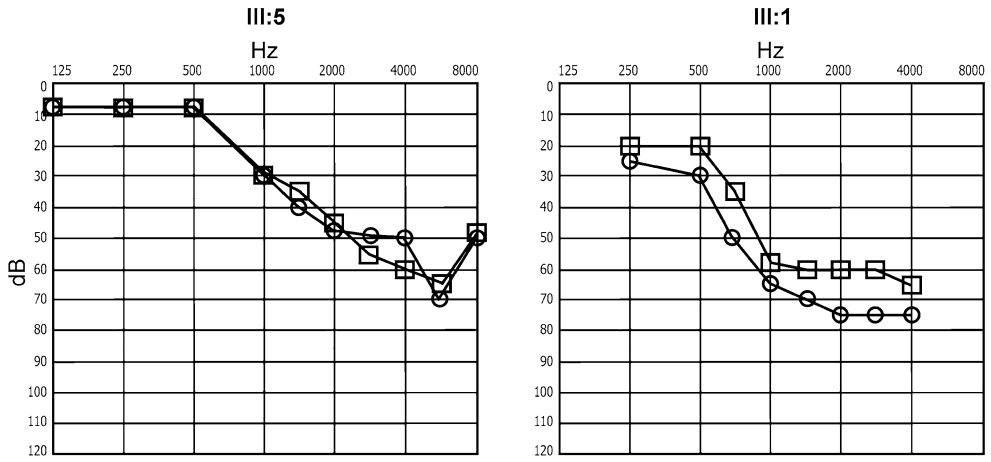

Fig. 1 *Left* Audiogram of the index patient, III:5, at the age of 30 years. Hearing is normal up to 500 Hz; at frequencies ≥500 Hz, there is a down-sloping configuration with maximum hearing loss at 6,000 Hz (65 dB on the *right* and 70 dB on the *left*, respectively). *Right* Audiogram of the index patient's affected sister, III:1, at the age of 41 years. Note that hearing loss is more advanced in III:1. *Circles* left ear, *squares* right ear

corrected visual acuity was 20/20 in both eyes. The anterior segments were normal. The vitreous showed liquefaction. Fundus examination (Fig. 2a, upper left panel) revealed mildly attenuated vessels and a normal optic disc appearance. In both eyes, there was little intraretinal bone spicule-like pigment clumping in the mid periphery. The right eye exhibited wrinkling of the inner limiting membrane due to a mild epiretinal membrane formation. Fundus autofluorescence imaging revealed spotted decreased autofluorescence in the mid periphery. The macular area exhibited mildly reduced autofluorescence surrounded by a ring of mildly increased autofluorescence (Fig. 2a, upper right panel). Kinetic perimetry revealed concentric symmetric restriction in both eyes with a preserved island for Goldmann II4e in the temporal periphery (Fig. 2b). In the dark-adapted scotopic electroretinogram (ERG), there was no signal detectable; the cone-driven photopic ERG (single-flash and 30 Hz flicker) showed only residual responses with markedly subnormal amplitudes in both eyes that were hardly distinguishable from noise (Fig. 2c). The patient's affected sister (III:1) had noticed impaired night vision at the age of 25 years and progressive glare sensitivity for the last 5 years. Best-corrected visual acuity was 20/20 in both eyes. Anterior segment examination revealed a mild posterior subcapsular cataract in both eyes. The vitreous showed liquefaction. Fundus features of typical retinitis pigmentosa were generally more apparent compared to her younger brother (III.5), including mildly to moderately attenuated vessels, waxy optic disc appearance and intraretinal bone spicule-like pigment clumping in the mid periphery (Fig. 2a, lower left panel). As in III:5, fundus autofluorescence imaging revealed spotted decreased autofluorescence in the mid periphery and mildly reduced autofluorescence surrounded by a ring of mildly increased autofluorescence in the macular area. However, in the mid periphery, the loss of autofluorescence was closer to the retinal center and more pronounced. Compared to III:5, the central area of reduced autofluorescence and the surrounding ring of increased autofluorescence were also smaller in diameter (Fig. 2a, lower right panel). Similar to III:5, kinetic perimetry showed symmetric restriction in both eyes with a preserved island for Goldmann II4e in the temporal periphery (Fig. 2b), and no signal was detectable in the scotopic ERG; the photopic ERG (single-flash and 30 Hz flicker) showed only residual responses with markedly subnormal amplitudes in both eyes (Fig. 2c). In summary, both individuals exhibited a phenotype of a rod-cone dystrophy with preserved visual acuity, concentric visual field loss, typical intraretinal pigment clumping in the mid periphery associated with signal reduction in fundus autofluorescence imaging. The findings in III:5 were generally less severe than in his 10 years elder sister (III:1), which is in line with a progressive panretinal dystrophy.

Linkage studies and mutation analysis

The most common USH2 locus, *USH2A*, could be excluded in this family as haplotypes were inconsistent with a mutation in the *USH2A* gene. Subsequent marker analyses also excluded the loci *USH1C*, *USH1D*, *USH1F*, *USH1G*, *USH2C*, and *USH3A* because haplotypes were inconsistent with a mutation in the corresponding genes (data not shown). As haplotypes were compatible with *USH1B*, and atypically mild Usher syndrome due to *MYO7A* mutations has been described previously (Liu et al. 1998), we performed mutation analysis for the complete *MYO7A* gene, but did not identify a causative mutation. Because of its putative interaction with the USH protein network, and with USH2A and VLGR1b in particular, we then considered whirlin as a possible candidate for USH2 in this family. Clearly, our family was too small for obtaining statistically significant linkage of the phenotype with any candidate locus (lod scores for informative microsatellite markers analysed ranged from 0.68 to 0.98). However, both patients in the family shared common haplotypes for markers of the *DFNB31* gene locus (Fig. 3a). We therefore performed sequence analysis for all 12 *DFNB31* exons including intron-exon boundaries and detected compound heterozygosity for a nonsense mutation, p.Q103X (c.307C>T), in exon 1 and a splice site mutation, c.837+1G>A, in the donor site of exon 2 (Fig. 3b). Both mutations show perfect segregation with the phenotype and were not detected in 100 healthy control individuals. Following the nomenclature for differentiation of genetic subtypes of Usher syndrome, we named this novel subtype, which is defined by mutations of the *DFNB31* gene on chromosome 9q32, *USH2D*. Because late-onset hearing loss segregates in an autosomal dominant pattern in the family of the patients' mother (II:2), who carries the c.837+1G>A splice site mutation, we sequenced exon 2 in her likewise affected brother, II:3. He does not carry the c.837+1G>A mutation.

We performed mutation screening of the complete *DFNB31* gene in an additional 96 USH2 patients of mostly European origin (including 24 Spanish individuals that have previously been excluded for mutations in exons 2–22 of the *USH2A* gene; all individuals have been excluded for the most common *USH2A* mutation,

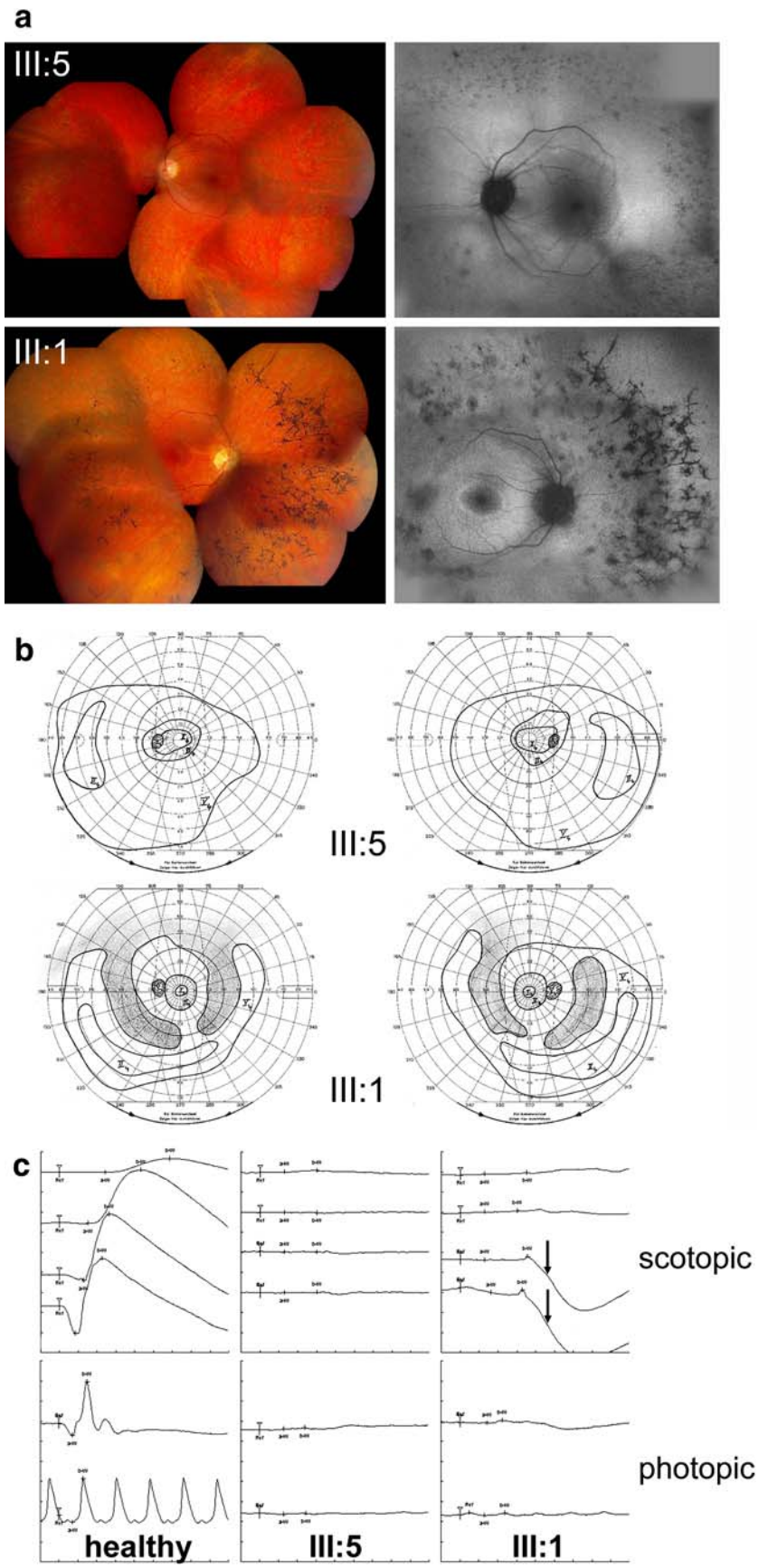

Fig. 2 **a** Composite image of the fundus photographs of the left eye of patient III:5 (*upper left panel*) and of the right eye of patient III:1 (*lower left panel*). Panoramic fundus autofluorescence images (ART modus of the HRA2) of the left eye of patient III:5 (*upper right panel*) and of the right eye of III:1 (*lower right panel*). **b** Kinetic monocular visual fields (Goldmann V4e, II4e, and I4e). **c** Electroretinographic responses in an unrelated healthy subject (*left*), patient III:5 (*middle*), and patient III:1 (*right*). For the scotopic ERG (*upper field*), responses to 36 and 24 db (scotopic standard ERG), 12 and 0 dB (maximal combined response) attenuation of the standard flash are shown. For the photopic ERG (*lower field*), responses to the standard flash and to 30 Hz flicker stimulation are shown. One unit on the *y*-axis represents 200 and 100 μV for the scotopic and photopic ERG, respectively. One unit on the *x*-axis represents 20 ms. The *arrows* (scotopic ERG in patient III:1) show blink artefacts

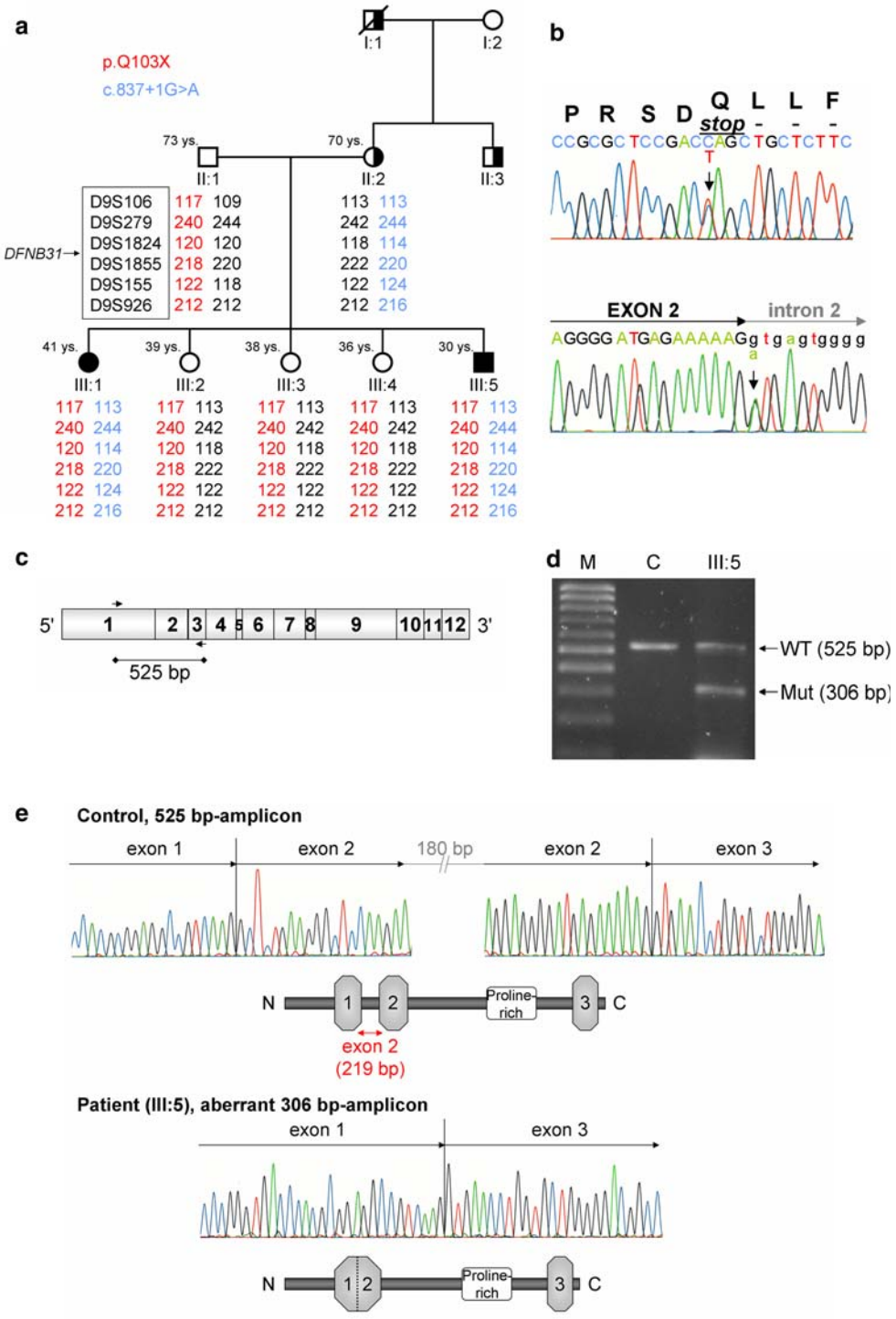

Fig. 3 **a** Pedigree of the *USH2D* family decribed herein. *Black symbols* congenital hearing loss and retinitis pigmentosa. *Half-filled symbols* progressive hearing loss with onset in third to sixth decade. III:5 index patient. Haplotypes are given for markers corresponding to the *DFNB31* locus (markers were selected from the UCSC Human Genome Browser). **b** *DFNB31* mutations identified in the USH2 family. An in-frame stop codon (p.Q103X) results from the transition c.307C>T in exon 1. The transition c.837+1G>A affects the invariant GT of the donor splice site consensus adjacent to exon 2. In a short N-terminal isoform of whirlin (GenBank AK056190), the latter alteration translates as a missense mutation, p.V280M. **c** Scheme of full-length *DFNB31* cDNA (drawn to scale; exons numbered from 1–12) with locations of primers used for RT-PCR. **d** RT-PCR analysis of the c.837+1G>A mutation: a segment of the *DFNB31* cDNA was amplified from whole blood of the index patient and an unaffected control (*C*). In addition to the 525 bp wild-type PCR product, the patient (who is heterozygous carrier of c.837+1G>A) shows an aberrant amplicon of 306 bp. *M* 100 bp DNA ladder. **e** Sequencing of both PCR products shown in **d** reveals normal splicing in the unaffected control, whereas in-frame skipping of exon 2 is seen in the index patient. The predicted Δexon-2-protein lacks the 3′ part of PDZ_1, the 5′ part of PDZ_2, and the linker region between them, leading to a fusion of PDZ_1 and PDZ_2

c.2299delG). No additional *DFNB31* mutations were identified.

Analysis of the splice site mutation c.837+1G>A

The c.837+1G>A mutation resulted in a smaller PCR product compared to the wild-type (Fig. 3d). Sequencing revealed in-frame skipping of exon 2 (219 bp), predicted to result in an aberrant long N-terminal isoform that lacks 73 residues, leading to a "fusion" of PDZ_1 and PDZ_2 that lack 9 and 11 residues in their C- and N-terminal parts, respectively, and the 53-residue linker region between them (Fig. 3e).

Discussion

Whirlin is the nearest homologue of the USH1C protein harmonin, possessing a similar modular structure with, depending on the isoform, up to three PDZ domains and a proline-rich domain. Mutations in the C-terminal half, thus affecting both the long and the short C-terminal isoform of whirlin (encoded by exon 1–12 and 6–12, respectively) have previously been reported to cause human non-syndromic deafness in humans (DFNB31; OMIM 607084) and in the whirler mouse (*wi*) (Mburu et al. 2003; Tlili et al. 2005). All DFNB31 and *wi* mutations described to date result in premature stop codons upstream of, or within, the region encoding PDZ_3. Through PDZ_1–PDZ_3, whirlin interacts with myosin-15a (MYO15a), a protein that is also involved in non-syndromic deafness. Both proteins, whirlin and myosin-15a, play a crucial role for developmental differential elongation of hair cell stereocilia (Belyantseva et al. 2005; Delprat et al. 2005; Kikkawa et al. 2005).

The long isoform of whirlin probably interacts with several proteins of the USH-network (Kremer et al. 2006). Whirlin colocalizes with two of these proteins, USH2A and VLGR1b (USH2C), in both, hair cell stereocilia and retinal photoreceptor cells. Applying a combination of a functional candidate approach and linkage studies, we show for the first time that whirlin mutations result in Usher syndrome type 2, from now on designated *USH2D*. While there are four genes (*MYO7A*, *CDH23*, *PCDH15*, and *USH1C*) in which allelic mutations either result in profound non-syndromic recessive deafness (DFNB) or the most severe subtype of Usher syndrome, USH1 (with profound deafness and RP (Ahmed et al. 2003)), we describe the first example of Usher syndrome type 2 allelic to non-syndromic deafness.

Strikingly, hearing impairment in our *USH2D* family (Fig. 1) is mild-to-moderate, in contrast to prelingual and profound deafness in the allelic non-syndromic disorder, DFNB31 (Mustapha et al. 2002). Hearing loss is significantly milder than has been described for the corresponding age groups of USH2 patients in general (Sadeghi et al. 2004). Moreover, and in contrast to the known DFNB-USH1 constellations, where in-frame changes result in DFNB and (mostly) truncating mutations cause USH1, both, DFNB31 and USH2D result from truncating mutations—but these are localized in different regions of the *DFNB31* gene (Fig. 4) (Mburu et al. 2003). We speculate that in both cases, the mutant messages may survive nonsense-mediated mRNA decay (in case of our family, this is suggested by the recovery of cDNA from

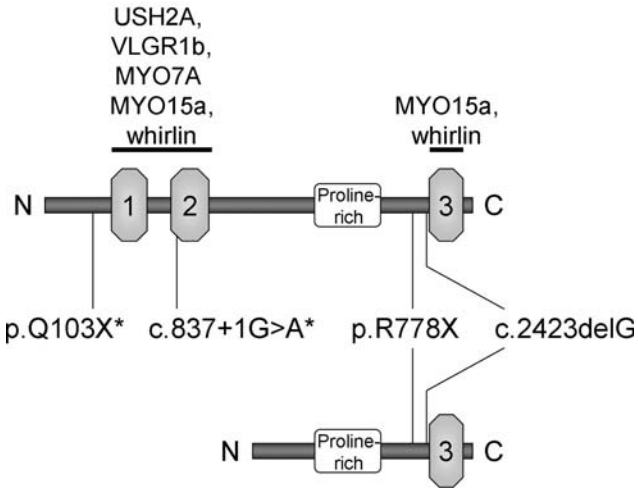

Fig. 4 Cartoon of the long (encoded by exons 1–12) and short C-terminal isoforms (ATG start codon in exon 6) of whirlin (drawn to scale). *Bars* indicate domains that may interact with proteins involved in Usher syndrome (USH2A, VLGRb1, MYO7A) and/or non-syndromic hearing impairment (MYO7A, MYO15a, whirlin). Localization of the USH2-related mutations identified in the family described herein (*) affect the long isoform, whereas DFNB31-related mutations are located in the C-terminal half of whirlin and hence affect both the long and the short C-terminal isoform

the mutant transcripts; Fig. 3d) and are translated to truncated proteins of different lengths. The phenotype (non-syndromic deafness vs. USH) may depend on the extent of the C-terminal truncation. The short C-terminal isoform (which is derived from an alternative start ATG in exon 6 and comprises the proline-rich domain and PDZ_3) is crucial for hearing, as it largely rescues the stereocilia growth and hearing defect in *wi* mice (Mburu et al. 2003). The existence of a comparable short isoform in humans has yet to be shown. In our *USH2D* family, mutations affect the long isoform of whirlin and are predicted to result either in truncation upstream of PDZ_1 and PDZ_2 (p.Q103X) or in a large in-frame deletion (c.837+1G>A). Of note, the latter alteration translates as a missense mutation, p.V280M, in a short N-terminal isoform of whirlin (GenBank AK056190 (Mburu et al. 2003)), consisting of exon 1 and an extended exon 2 (on the 3′ end, 201 bp are included as the c.837+1G donor site is not used). The short C-terminal isoform is predicted to remain preserved (assuming its existence in humans), which could explain the mild-to-moderate hearing deficit instead of profound deafness in our family (however, we can not rule out that expression of the short C-terminal isoform is altered). This indicates that the N-terminal domains, PDZ_1 and PDZ_2, also play a role in hearing (which is reflected by the fact that outer hair cells still

have mildly abnormal morphology in the *wi* mice rescue experiment mentioned above (Mburu et al. 2003)), but to a lesser extent than the C-terminal isoform. Loss or structural impairment of the N-terminal PDZ_1 and PDZ_2 domains, however, results in a visual phenotype. We therefore speculate that the interaction of whirlin with the USH2 proteins USH2A and VLGR1b, which is mediated by PDZ_1 and PDZ_2 (Adato et al. 2005; van Wijk et al. 2006), is crucial for both, normal hearing and retinal integrity in particular. This hypothesis is in line with the lack of a retinal phenotype in both, DFNB31 individuals and the *wi* mouse. Nevertheless, subclinical or mild retinal dysfunction should be excluded in the DFNB31 patients reported to date by detailed ophthalmological investigation. We assume that only exons 1–6 of *DFNB31* are candidate regions for mutations in USH2 patients although, for the time being, exons 7–12 should be investigated as well. Further mutation screening in USH2 patients has to be done in order to support this proposed genotype-phenotype correlation. It cannot be excluded that truncations on both *DFNB31* alleles result in a more severe phenotype. However, van Wijk et al. (2006) did not identify any disease-causing *DFNB31* mutations in 20 USH1 patients.

Because late-onset hearing loss was reported for the family of the index patient's mother in at least two generations, we hypothesized that heterozygosity for the *DFNB31* mutation contributed by II:2, c.837+1G>A, may impair hearing. However, as her affected brother, II:3, does not carry this mutation, a genetic cause other than whirlin is probably responsible for the auditory phenotype in the mother's family.

We show that *DFNB31* is the ninth gene that is involved in Usher syndrome. Our findings demonstrate the usefulness of a functional candidate approach in the identification of novel USH genes.

Acknowledgments Supported by grants BO 2954/1-1 (Deutsche Forschungsgemeinschaft) and Koeln Fortune Program, grant 113/2004 (Faculty of Medicine, University of Cologne), to H.B., and by Heisenberg fellowship SCHO 734/2-1 (Deutsche Forschungsgemeinschaft) and EU FP6, Integrated Project "EVIGENORET" (LSHG-CT-2005-512036), to H.P.N.S. We are indebted to the family who has participated in this study.

References

Adato A, Lefevre G, Delprat B, Michel V, Michalski N, Chardenoux S, Weil D, El-Amraoui A, Petit C (2005) Usherin, the defective protein in Usher syndrome type IIA, is likely to be a component of interstereocilia ankle links in the inner ear sensory cells. Hum Mol Genet 14:3921–3932

Ahmed ZM, Riazuddin S, Wilcox ER (2003) The molecular genetics of Usher syndrome. Clin Genet 63:431–444

Belyantseva IA, Boger ET, Naz S, Frolenkov GI, Sellers JR, Ahmed ZM, Griffith AJ, Friedman TB (2005) Myosin-XVa is required for tip localization of whirlin and differential elongation of hair-cell stereocilia. Nat Cell Biol 7:148–156

Ben-Yosef T, Ness SL, Madeo AC, Bar-Lev A, Wolfman JH, Ahmed ZM, Desnick RJ, Willner JP, Avraham KB, Ostrer H, Oddoux C, Griffith AJ, Friedman TB (2003) A mutation of PCDH15 among Ashkenazi Jews with the type 1 Usher syndrome. N Engl J Med 348:1664–1670

Bitner-Glindzicz M, Lindley KJ, Rutland P, Blaydon D, Smith VV, Milla PJ, Hussain K, Furth-Lavi J, Cosgrove KE, Shepherd RM, Barnes PD, O'Brien RE, Farndon PA, Sowden J, Liu XZ, Scanlan MJ, Malcolm S, Dunne MJ, Aynsley-Green A, Glaser B (2000) A recessive contiguous gene deletion causing infantile hyperinsulinism, enteropathy and deafness identifies the Usher type 1C gene. Nat Genet 26:56–60

Delprat B, Michel V, Goodyear R, Yamasaki Y, Michalski N, El-Amraoui A, Perfettini I, Legrain P, Richardson G, Hardelin JP, Petit C (2005) Myosin XVa and whirlin, two deafness gene products required for hair bundle growth, are located at the stereocilia tips and interact directly. Hum Mol Genet 14:401–410

Hope CI, Bundey S, Proops D, Fielder AR (1997) Usher syndrome in the city of Birmingham–prevalence and clinical classification. Br J Ophthalmol 81:46–53

Keats BJ, Corey DP (1999) The usher syndromes. Am J Med Genet 89:158–166

Kikkawa Y, Mburu P, Morse S, Kominami R, Townsend S, Brown SD (2005) Mutant analysis reveals whirlin as a dynamic organizer in the growing hair cell stereocilium. Hum Mol Genet 14:391–400

Kremer H, van Wijk E, Marker T, Wolfrum U, Roepman R (2006) Usher syndrome: molecular links of pathogenesis, proteins and pathways. Hum Mol Genet 15(Suppl 2):R262–270

Liu XZ, Hope C, Walsh J, Newton V, Ke XM, Liang CY, Xu LR, Zhou JM, Trump D, Steel KP, Bundey S, Brown SD (1998) Mutations in the myosin VIIA gene cause a wide phenotypic spectrum, including atypical Usher syndrome. Am J Hum Genet 63:909–912

Marmor MF, Holder GE, Seeliger MW, Yamamoto S (2004) Standard for clinical electroretinography (2004 update). Doc Ophthalmol 108:107–114

Mburu P, Mustapha M, Varela A, Weil D, El-Amraoui A, Holme RH, Rump A, Hardisty RE, Blanchard S, Coimbra RS, Perfettini I, Parkinson N, Mallon AM, Glenister P, Rogers MJ, Paige AJ, Moir L, Clay J, Rosenthal A, Liu XZ, Blanco G, Steel KP, Petit C, Brown SD (2003) Defects in whirlin, a PDZ domain molecule involved in stereocilia elongation, cause deafness in the whirler mouse and families with DFNB31. Nat Genet 34:421–428

Mustapha M, Chouery E, Chardenoux S, Naboulsi M, Paronnaud J, Lemainque A, Megarbane A, Loiselet J, Weil D, Lathrop M, Petit C (2002) DFNB31, a recessive form of sensorineural hearing loss, maps to chromosome 9q32–34. Eur J Hum Genet 10:210–212

Ness SL, Ben-Yosef T, Bar-Lev A, Madeo AC, Brewer CC, Avraham KB, Kornreich R, Desnick RJ, Willner JP, Friedman TB, Griffith AJ (2003) Genetic homogeneity and phenotypic variability among Ashkenazi Jews with Usher syndrome type III. J Med Genet 40:767–772

Pennings RJ, Te Brinke H, Weston MD, Claassen A, Orten DJ, Weekamp H, Van Aarem A, Huygen PL, Deutman AF, Hoefsloot LH, Cremers FP, Cremers CW, Kimberling WJ, Kremer H (2004) USH2A mutation analysis in 70 Dutch families with Usher syndrome type II. Hum Mutat 24:185

Rosenberg T, Haim M, Hauch AM, Parving A (1997) The prevalence of Usher syndrome and other retinal dystrophy-hearing impairment associations. Clin Genet 51:314–321

Sadeghi M, Cohn ES, Kelly WJ, Kimberling WJ, Tranebjoerg L, Moller C (2004) Audiological findings in Usher syndrome types IIa and II (non-IIa). Int J Audiol 43:136–143

Spandau UH, Rohrschneider K (2002) Prevalence and geographical distribution of Usher syndrome in Germany. Graefes Arch Clin Exp Ophthalmol 240:495–498

Tlili A, Charfedine I, Lahmar I, Benzina Z, Mohamed BA, Weil D, Idriss N, Drira M, Masmoudi S, Ayadi H (2005) Identification of a novel frameshift mutation in the DFNB31/WHRN gene in a Tunisian consanguineous family with hereditary non-syndromic recessive hearing loss. Hum Mutat 25:503

van Wijk E, van der Zwaag B, Peters T, Zimmermann U, Te Brinke H, Kersten FF, Marker T, Aller E, Hoefsloot LH, Cremers CW, Cremers FP, Wolfrum U, Knipper M, Roepman R, Kremer H (2006) The DFNB31 gene product whirlin connects to the Usher protein network in the cochlea and retina by direct association with USH2A and VLGR1. Hum Mol Genet 15:751–765

Verpy E, Leibovici M, Zwaenepoel I, Liu XZ, Gal A, Salem N, Mansour A, Blanchard S, Kobayashi I, Keats BJ, Slim R, Petit C (2000) A defect in harmonin, a PDZ domain-containing protein expressed in the inner ear sensory hair cells, underlies Usher syndrome type 1C. Nat Genet 26:51–55